Comparison of Cooling Technologies for Transport Logistics

Sebastian Leopoldus[1*], Alessandro Consolati[2], Prof. Dr. Peter Radgen[1], Prof. Dr. Simone Zanoni[2]

[1] Institute of Energy Economics and Rational Energy Use, University of Stuttgart, Heßbrühlstraße 49a, DE-70565 Stuttgart
[2] Department of Mechanical and Industrial Engineering, University of Brescia, Via Branze 38, IT-25123 Brescia
[*]Email: sebastian.leopoldus@ier.uni-stuttgart.de

Abstract

Despite efforts to increase energy efficiency, the final energy consumption for freight transport in Europe constantly increased during the last years. Food, beverages, and tobacco accounts for the largest share of tonne-kilometres in road freight transport, while about one-third of the transported products require refrigeration or cooling. Standard technology today are vapour-compression refrigeration (VCR) systems operated either via the vehicle engine or with a dedicated diesel engine, both increasing the fuel consumption for transportation. To achieve the energy and climate targets of the EU, further research is needed for the transport sector and especially on alternative cooling technologies in transportation applications, which are more efficient, and/or using renewable energy.

This paper will present an evaluation of different alternative refrigeration technologies such as (i) eutectic cooling by the use of phase change materials (PCM), (ii) cryogenic cooling, (iii) solid oxide fuel cell in combination with vapour absorption refrigeration, and (iv) photovoltaic (PV) cells as an energy provider for the vapour compression refrigeration (VCR).

The alternative systems are compared to the VCR systems regarding technical feasibility, GHG-emissions, and economic competitiveness (investment and operational cost). Required cooling loads are calculated for different truck sizes and distribution scenarios as well as solar potentials in different regions of Europe. Emissions during operation as well as emissions related to the production and losses of the fuels and refrigerants are taken into account. However, emissions related to the production of the required hardware are not considered.

The results show that all the alternative technologies are feasible, except for the PV-driven VCR system, which alone cannot provide enough energy during some months or transport scenarios. They might need to be supplemented by an energy storage device. However, PV-driven VCR and eutectic cooling seem to be the most promising systems in terms of emission reduction potential.

Introduction

The most common way to transport food in need of refrigeration on land is to use refrigerated trucks. The trucks connect the different stages of the cold supply chain. Due to demographic changes, the total number of refrigerated vehicles around the world is estimated to reach 15.5 million by 2025, up from 3 million in 2013 (Automotive Fleet 2015). The vapour-compression refrigeration (VCR) system is the most common technology for on-road mobile refrigeration applications and 90% of these systems are operated via a dedicated diesel engine (Rai and Tassou 2017b). The diesel engine, with a typical fuel consumption of 0.47 l/h per kW cooling capacity (Liu et al. 2012), emits greenhouse gases (GHG), particulate matter and nitrogen oxides (NOx) which have a negative impact on the environment. Regarding the energy and climate targets of the EU, there is a need to establish alternative technologies for mobile cooling applications with less environmental impact. This work presents a comparison of some alternative cooling technologies for transport logistics regarding technical applicability, environmental impact and economic competitiveness.

Alternative refrigeration systems for transport applications

In this work the following four refrigeration systems are analysed:

1. Eutectic cooling

2. Cryogenic cooling
3. PV cells in combination with vapour compression refrigeration (VCR)
4. Solid oxide fuel cell (SOFC) in combination with a vapour absorption refrigeration system (VARS)

The eutectic and cryogenic systems are alternative technologies, while the fuel cell and PV cells are only an alternative energy supply for the absorption and compression refrigeration systems, respectively.

Eutectic cooling

The eutectic cooling system consists of hollow tubes, beams or plates filled with a eutectic solution (phase change material – PCM) (Tassou et al. 2009). During operation, a charging phase and a discharging phase alternate, with the PCM acting as energy storage. First, the system must be charged off-vehicle, which means that heat is removed from the phase change material and the phase change material transitions from liquid to solid phase. For this charging phase, a stationary compression refrigeration system can be used to transfer the heat from the phase change material to the environment. When the truck is in operation, cooling is provided by discharging the phase change material. By absorbing heat from the cooling compartment of the truck, the PCM changes its phase from solid to liquid and therefore providing the cooling effect to the refrigerated space of the truck. When all the PCM has changed to the liquid phase, the system needs to be recharged. Liu et al. (2012) developed a novel design of refrigerated trucks consisting of an off-vehicle refrigeration unit with an on-vehicle PCM storage unit. There are two main factors to consider when selecting suitable PCMs: The melting point and the enthalpy of fusion. To keep the required heat transfer area within the refrigerated space as small as possible, the melting point should be as low as possible. However, if the melting point is chosen too low, the off-vehicle refrigeration unit will be more expensive and operate at lower efficiency (Liu et al. 2012). The higher the specific enthalpy of fusion, the less mass of PCM is needed to provide a certain cooling capacity. Bonaventure et al. (2020) studied the configuration of the eutectic plates on a truck to optimize the refrigeration and Radebe et al. (2020) designed a physical and mathematical model on the utilization of eutectic plates on medium refrigeration transport. They found a good performance of the system when working between -18°C and 0°C with an ambient temperature of 25°C.

Cryogenic cooling

Cryogenic cooling is achieved by the evaporation of cryogenic liquids. Low-temperature liquids are taking up heat leading to the evaporation of the cryogenic liquid. The temperature at which the phase change takes place is determined by the pressure in the systems. The energy required for this phase transition is withdrawn from the cooling compartment of the truck. The most commonly used cryogenic fluids are liquid nitrogen and carbon dioxide. These gases are stored in tanks underneath the vehicle and are either sprayed directly into the refrigerated space and evaporated there or, in the case of safety concerns, evaporated in an evaporator coil to cool the air inside the refrigerated space. In the latter case, the cryogenic fluid is released into the environment via an exhaust system. (Thermo King 2014).

Although cryogenic fluids were identified as an alternative technology more than 40 years ago, they have not yet achieved a significant market share in transport applications despite very low temperatures such as required e.g. for the transportation of COVID-19 vaccinations. The reasons for this are the high cost of the production of the cryogenic fluids using electricity compared to the use of fossil fuels, limited availability of the fluids and limited storage capacity for cryogenic liquids due to the cost of cryogenic tanks (Pedolsky and La Bau 2010). A study has been carried out to compare cryogenic cooling to the state of the art VCR system in terms of greenhouse gas (GHG) emissions (Rai and Tassou 2017a). The authors found that although the GHG emissions of the cryogenic application are lower during operation, the overall emissions including the production of the cryogenic liquids are similar. A comparison of different cryogenic fluids varying different parameters such as vehicle size, cooling temperature and delivery conditions shows that tank size can be a limiting factor for long-distance delivery (Rai and Tassou 2017b).

PV cells with vapour compression refrigeration

Photovoltaic cells generate electricity by absorbing sunlight. In combination with the VCR system, the generated electricity is used to power the compressor of the refrigeration cycle via an electric motor. The main advantages of the PV technology are the clean and silent operation as well as the modularity, which makes them flexible in terms of total energy production. However, the electricity generated by the PV cells is highly dependent on external influences and seasonal factors. Kühnel et al. (2017) studied the electricity production of a vehicle integrated PV system with a focus on trucks for cooling applications. They operated three large trucks in Germany with two different kinds of PV panels covering an area on the roof of 28m² and 33m², respectively, which produced 3-7 MWh/year of net electricity per vehicle resulting in annual CO_2 savings of 1-2 tonnes per

vehicle. Mak et al. (2017) conducted an experiment with four PV panels either powering the compressor of the refrigeration cycle or a battery pack and refrigeration temperatures down to -24°C could be provided with light goods load. Eitner et al. (2020) have analysed that diesel savings of up to 2113 l/year can be achieved based on an experiment measuring 6 refrigerated trucks powered by rooftop PV cells in Europe and North America.

Solid oxide fuel cell with vapour absorption refrigeration

The vapour absorption refrigeration system (VARS) is similar to the vapour compression system, but the mechanical compressor is replaced by a thermal compressor using a sorbent. Instead of electrical power, a heat source provides the required energy to compress the working fluid of the refrigeration system. The thermal compression is carried out through a mechanism of absorption and desorption in an absorber and desorber (generator), respectively, resulting in a concentration change of the solution. A solution pump, solution valve and a solution heat exchanger (SHX) serve as supporting components (Ariyadi 2016).

The fuel cell generates electrical energy through a chemical reaction, whereby various feedstocks such as hydrogen, methanol, methane, etc. can be used. Fuel cell technology is becoming increasingly important because it generally emits fewer GHG emissions than fossil-fuelled combustion engines due to its higher efficiency. The modularity and silent operation of the fuel cell are additional benefits. In principle, the fuel cell can provide electricity for operating electrical devices on the truck and the drive train. In addition, it provides waste heat to drive the absorption refrigeration cycle. Garde et al. (2012) developed a fuel-cell based refrigeration system using hydrogen as a fuel and carried out a feasibility study for two different delivery scenarios. The study shows that the developed system is technically feasible and the refrigeration requirements could be satisfied under the analysed scenarios. Brooks et al. (2016) also designed a system using hydrogen-powered fuel cells and compared the fuel cells of two different manufacturers. A long-term study with an operation time of 1000 hours was carried out. (Venkataraman et al. 2016) demonstrated the coupling of a solid oxide fuel cell (SOFC) with a vapour absorption refrigeration system (VARS) recycling the heat generated by the SOFC and using it to power the VARS. Pandya et al. (2020) shows that the SOFC-coupled VARS has significantly lower GHG emissions compared to diesel-driven VCR.

Calculations for the comparison of the alternative technologies

In the following section, the approach for calculating the cooling loads as a monthly average in the different scenarios (see chapter Scenario definition) is described. Based on this approach, the annual GHG emissions are calculated for the different technologies, distinguishing between operational emissions and the emissions related to the production of the working fluids. For the economic analysis, the net present value (NPV) (Belyadi et al. 2019) is calculated for each technology, considering the annual operation costs, investment costs and savings on taxes, assuming a discount rate of 4%, a taxation of 27% and a depreciation time of 6 years for all systems.

Average cooling load

The approach for calculating the cooling load is based on Venkataraman et al. (2016) with some minor changes that are explained for the respective equation. The total cooling load of a refrigerated truck depends on many factors like required cooling temperature, ambient temperature, insulation, number and size of doors, number and duration of door openings during operation and the dimension of the trailer. The total heat load Q_{total} as an average of each month for a given scenario can defined as followed.

$$Q_{total} = Q_{THL} + Q_{SHL} + Q_{SL} + Q_{PHL} \quad (1)$$

It is calculated as the sum of transmission heat load (THL), service heat load (SHL), solar heat load (SL) and product heat load (PHL) (Venkataraman et al. 2016). The THL describes the amount of energy that penetrates the refrigerated space according to Fourier's law:

$$Q_{THL} = k_b * A_{mean} * \Delta T. \quad (2)$$

In this equation, k_b is the thermal transmittance of the refrigerated trailer (body) including the convective heat transfer between the inner wall and the air in the cooling compartment, A_{mean} is the mean surface area of the refrigerated space and ΔT is the temperature difference between the ambient temperature and the refrigerated space. The SHL

$$Q_{SHL} = K * A_c * V_t * \left(\frac{h_a}{v_a} - \frac{h_r}{v_r}\right) * \left(\frac{60}{t_{avg}}\right) * X \quad (3)$$

describes the energy intake caused by door openings, where K describes the ratio of actual enthalpy change to maximum theoretical enthalpy change, A_c is the number of air changes inside the refrigerated space resulting from door openings, V_t being the internal volume of the trailer minus the volume occupied by the products, with the specific volumes v of ambient and refrigerated air, respectively and h being their respective enthalpy. t_{avg} is the average time between two door openings and X is a factor fitted from experimental data. For more detailed information on this calculation, the reader is referred to Venkataraman et al. (2016). The SL

$$Q_{SL} = k * A_{solar} * (T_{solar} - T_r) \tag{4}$$

is the amount of heat penetrating the refrigerated space due to solar insolation, where k is the overall heat transfer coefficient, A_{solar} is the outside area of the refrigerated area that is exposed to the sun, T_r is the refrigeration temperature and

$$T_{solar} = T_a + \frac{\phi * \tilde{\alpha}}{\alpha_{out}} \tag{5}$$

is the mean solar air temperature. In equation (5), T_a is the temperature of the ambient air, $\tilde{\alpha}$ is the surface absorptivity of the outside material of the truck, α_{out} is the outside heat transfer coefficient and

$$\phi_i = \frac{\frac{\phi_{i,1} + \phi_{i,15} + \phi_{i,30}}{3\ days} * 24 \frac{hours}{day}}{t_{op}} \tag{6}$$

is the average solar radiation, which differs from the approach of Venkataraman et al. (2016), who did not consider its monthly dependence. The average solar insolation is different for every month $i = \{Jan, Feb, \dots, Dec\}$ and an average is calculated using the average daily radiation for day 1, 15 and 30 of each month. t_{op} is the amount of operating hours for one day. The values for the respective solar radiation are taken from a database (Honsberg and Bowden 2019). The PHL is the heat load related to cooling the products on the truck if they are loaded at a temperature above the temperature of the cooling compartment of the truck. Since it is assumed that the products are loaded at the refrigeration temperature (see chapter Scenario definition), the PHL is zero and can therefore be neglected. The accumulated annual cooling energy is expressed as the sum of the cooling loads per month ($E_C = \sum_{i=1}^{12} Q_{total,i} * t_{op} * n_d$), with n_d being the number of days the systems are operated each month.

Vapour compression system (VCR)

The VCR system traditionally used for cooling of refrigerated trucks consists of the main components compressor, condenser, evaporator and expansion valve. The required energy is provided by a diesel engine.

To estimate the environmental impact of this system, the annual greenhouse gas emissions (GHG) are calculated for the operation of the system as well as for the production of the diesel and the refrigerant (R452A) according to equations (7) and (8)

$$GHG_{op,VCR} = GHG_{op,diesel} + GHG_{op,ref} \tag{7}$$

$$GHG_{prod,VCR} = GHG_{prod,diesel} + GHG_{prod,ref}. \tag{8}$$

The GHG emissions related to the operation of the diesel engine are calculated by multiplying the annual required mass of diesel with the emission factor ($EF = 2.7\ kgCO_2e/l$) for diesel (Department for Business, Energy & Industrial Strategy 2017).

$$GHG_{op,diesel} = V_{diesel} * EF_{diesel} = \frac{m_{diesel}}{\rho_{diesel}} * EF_{diesel} \tag{9}$$

The annual mass of diesel required is calculated according to equation (10) by dividing the annual amount of energy required for cooling by the amount of energy provided per kg of diesel. The energy intensity of diesel is $h_{\text{diesel}} = 11.8\ kWh\ kg^{-1}$. It is assumed that the efficiency of the motor is at 20% and two-thirds of the work is usable to operate the VCR system, while one-third is used to run the ancillary systems (Rai and Tassou 2017b).

$$m_{diesel} = \frac{E_C}{h_{diesel} * 0.2 * 2/3} \tag{10}$$

The operational GHG emissions of the refrigerant are related to its leakage. Using the typical total amount of refrigerant in the system ($m_{\mathrm{ref}} = 5\ kg$) (Thermo King n.d.) with a leakage of 2% per year (Wu et al. 2013) and the global warming potential for the refrigerant R452A ($GWP_{\mathrm{ref}} = 2140\ kgCO_2e/kg$) (California Air Resources Board n.d.), the operational GHG emissions of the refrigerant can be calculated according to equation (11)

$$GHG_{op,ref} = m_{ref,leak} * GWP_{ref} = m_{ref} * 2\% * GWP_{ref}. \tag{11}$$

The GHG emissions related to the production of the diesel and refrigerant are calculated according to equations (12) and (13) using the emission factors for the production of diesel ($EFP_{\mathrm{diesel}} = 0.93\ kgCO_2e/l$) (Eriksson and Ahlgren 2013) and R452A ($EFP_{\mathrm{ref}} = 0.21\ kgCO_2e/kg$) (Rai and Tassou 2017b)

$$GHG_{prod,diesel} = V_{diesel} * EFP_{diesel} = \frac{m_{diesel}}{\rho_{diesel}} * EFP_{diesel} \tag{12}$$

$$GHG_{prod,ref} = \left(m_{ref} + m_{ref,leak}\right) * EFP_{ref}. \tag{13}$$

The operation costs ($C_{\mathrm{op,VCR}}$) are calculated by multiplying the costs of diesel ($c_{\mathrm{diesel}} = 1.50\ €/l$) and refrigerant ($c_{\mathrm{ref}} = 50\ €/kg$) with the respective annually required masses

$$C_{op,VCR} = m_{diesel} * c_{diesel} + m_{ref,leak} * c_{ref}. \tag{14}$$

The investment costs ($C_{\mathrm{inv,VCR}}$) are calculated using typical investment costs for diesel driven transport refrigeration units ($C_{\mathrm{VCR}} = 20{,}000€$) (Air Resources Board 2015) and the initially required mass of refrigerant with its cost

$$C_{inv,VCR} = C_{VCR} + m_{ref} * c_{ref}. \tag{15}$$

Eutectic system

The eutectic system consists of an on-vehicle phase change thermal storage unit (PCTSU) located outside the refrigerated space, an off-vehicle refrigeration unit (VCR) powered by electricity, a cooling unit inside the refrigerated space and some auxiliary units (Liu et al. 2012). The specific energy of the phase change material (PCM) is calculated according to equation (16)

$$h_{PCM} = \frac{H_{PCM,L}}{m_{PCM,L}} \tag{16}$$

where $H_{\mathrm{PCM,L}} = 40\ MJ$ is the net amount of energy provided by the PCM before it has to be recharged and $m_{\mathrm{PCM,L}} = 360\ kg$ is the total mass of PCM inside the PCTSU in the scenario of Liu et al. (2012). The mass flow of PCM ($\dot{m}_{\mathrm{PCM,i}}$) for a certain month is then calculated by dividing the total cooling load required in a given scenario by the specific energy of the PCM

$$\dot{m}_{PCM,i} = \frac{Q_{total,i}}{h_{PCM}} \tag{17}$$

The mass of PCM that is required daily during a certain month in the scenarios of this work (m_{PCM}) is calculated as follows:

$$m_{PCM,i} = \dot{m}_{PCM,i} * t_{op}. \tag{18}$$

The GHG emissions related to the leakage of the off-vehicle VCR system are calculated following equation (11) and it is assumed that there are no operation-related PCM emissions. The production-related GHG emissions are divided into production of electricity to power the off-vehicle VCR system, production of the refrigerant and production of the PCM

$$GHG_{prod,eut} = GHG_{prod,el} + GHG_{prod,ref} + GHG_{prod,PCM}. \tag{19}$$

The production-related GHG emissions for electricity are calculated according to equation (20)

$$GHG_{prod,el} = \frac{E_C}{COP_{total,eut}} * EFP_{el} \quad (20)$$

where $EFP_{\mathrm{el}} = 0.401\, kgCO_2e/kWh$ (Umweltbundesamt 2020) is the emission factor for electricity in Germany in 2019 and $COP_{\mathrm{total,eut}} = COP_{\mathrm{PCTSU}} * COP_{\mathrm{VCR}}$ is the total Coefficient Of Performance (COP) of the system with $COP_{\mathrm{PCTSU}} = 0.72$ (Liu et al. 2012) being the COP of the storage unit and $COP_{\mathrm{VCR}} = 2.50$ (own assumption) being the COP of the off-vehicle VCR. $GHG_{\mathrm{prod,ref}}$ is calculated following equation (13) and $GHG_{\mathrm{prod,PCM}}$ is calculated according to equation (21)

$$GHG_{prod,PCM} = EFP_{PCM} * 2\left(max\{m_{PCM,i}\} + m_{PCM,leak}\right) = EFP_{PCM} * 2\left(max\{m_{PCM,i}\}(1 + 2\%)\right). \quad (21)$$

$EFP_{\mathrm{PCM}} = 0.006\, kgCO_2e/kg$ (Phase Change Material Products Limited n.d.) is the emission factor for the production of PCM which needs to be replaced twice a year and a loss of 2% is assumed. The max function is used to represent the worst-case scenario, which corresponds to the month in which the required mass of PCM is at a maximum.

The operation costs ($C_{\mathrm{op,eut}}$) consist of the electricity cost to power the off-vehicle VCR and the cost for the annual demand of refrigerant and PCM

$$C_{op,eut} = \left(max\{m_{PCM,i}\}(1 + 2\%)\right) * c_{PCM} * 2 + m_{ref,leak} * c_{ref} + \frac{CL}{COP_{total,eut}} * c_{el} \quad (22)$$

where $c_{\mathrm{PCM}} = 1\,€/kg$ (Phase Change Material Products Limited n.d.) is the cost of PCM and $c_{\mathrm{el}} = 0.178\,€/kWh$ (BDEW 2021) is the average cost for electricity in Germany. The investment costs ($C_{\mathrm{inv,eut}}$) consist of the costs for the on-vehicle eutectic system and the off-vehicle VCR system

$$C_{\mathrm{inv,eut}} = n_{\mathrm{plate}} * c_{\mathrm{plate}} + C_{\mathrm{VCR,stat}} = \frac{\max\{m_{\mathrm{PCM},i}\}}{m_{\mathrm{PCM,plate}}} * c_{\mathrm{plate}} + C_{\mathrm{VCR,stat}} \quad (23)$$

where n_{plate} is the number of eutectic plates required inside the PCTSU, $c_{plate} = 400€$ is the cost for one plate and $m_{PCM,plate} = 88\ kg$ (FIC S.p.A. n.d.) is the amount of PCM that can be stored in one plate. $C_{VCR,stat} = 15{,}000€$ (own assumption based on Rai and Tassou (2017b)) is the cost for the off-vehicle VCR system.

Cryogenic system

The cryogenic system consists of a cryogenic fuel tank from which the cryogenic liquid is pumped to the sprayer units, which feed the liquid to the refrigerated space where it is vaporised to achieve the cooling effect. The energy required for the pump is very small and not considered in the calculations. For this system, liquid CO_2 (LCO_2) and liquid N_2 (LN_2) are considered.

The required mass flows of the cryogenic fluids are calculated using the energy balances according to equation (24).

$$\dot{m}_{j,i} = \frac{Q_{total,i}}{\Delta h_{v,j} + c_{p,j} * \left(T_r - T_{v,j}\right)} \quad (24)$$

$\dot{m}_{j,i}$ is the mass flow for the fluid $j = \{\mathrm{LCO_2}, \mathrm{LN_2}\}$ in a certain month i in the scenarios, $\Delta h_{v,j}$ is the respective evaporation enthalpy, $c_{p,j}$ is the respective heat capacity and $T_{v,j}$ is the respective evaporation temperature.

For the calculation of the GHG emissions it is assumed that there are no operation-related emissions, because both LCO_2 and LN_2 are recovered and then released to the atmosphere after their use (Rai and Tassou 2017b). The annual production-related GHG emissions are calculated using the respective emission factor ($EFP_{\mathrm{LCO_2}} = 0.305\ kgCO_2e/kg$, $EFP_{\mathrm{LN_2}} = 0.254\ kgCO_2e/kg$) (Rai and Tassou 2017b) for production.

$$GHG_{prod,j} = EFP_j * \sum_{i=1}^{12} \dot{m}_{j,i} * t_{op} * n_d \quad (25)$$

The operation costs are calculated using equation (26) with costs of $c_{\mathrm{LCO_2}} = 0.12\,€/kg$ and $c_{\mathrm{LN_2}} = 0.08\,€/kg$, respectively (Rai and Tassou 2017b).

$$C_{op,j} = c_j * \sum_{i=1}^{12} \dot{m}_{j,i} * t_{op} * n_d \quad (26)$$

The investment costs are different depending on truck size. This is represented by the size factor F which is equal to 1 for large trucks and 0.8 for medium size trucks. Typical investment costs for a cryogenic cooling system for large trucks are $C_{\text{cryo}} = 22{,}000$ € (Rai and Tassou 2017b)

$$C_{inv,cryo} = C_{cryo} * F. \quad (27)$$

Vapour absorption refrigeration system (VARS) powered by solid oxide fuel cell (SOFC)

The VARS+SOFC system consists of two systems that are thermally coupled using a thermal oil circuit. The chemical reaction of water and natural gas in the fuel cell generates direct current, which is used to power various electricity consumers on the truck, and heat at about 700-800°C. The heat produced is used in the desorber of the solution circuit (NH_3-H_2O solution) of the VARS system (Venkataraman et al. 2016). The solution circuit consisting of desorber, absorber, solvent pump and expansion valve functions as a thermal compressor analogous to the mechanical compressor in a VCR to power the refrigeration cycle.

The necessary mass flow of natural gas to provide the required cooling capacity in a certain month can be calculated according to equation (28), where $Q_{\text{SOFC},i}$ is the required power input for the SOFC system, $LHV_{\text{CH}_4} = 15.3\,kWh/kg$ is the lower heating value of methane and $\eta_{\text{co}} = 0.46$ and $\eta_{\text{el}} = 0.35$ are the cogeneration and the electrical efficiencies. By calculating the difference between the two efficiencies, only the heat provided is taken into account. Although we believe that the efficiency for cogeneration should be higher, the values are based on the results of Pandya et al. (2020), who define a benefit function to find the optimal operating parameters.

$$\dot{m}_{CH_4,i} = \frac{Q_{SOFC,i}}{LHV_{CH_4}} = \frac{Q_{total,i}}{\eta_{co} - \eta_{el}} * \frac{1}{LHV_{CH_4}} \quad (28)$$

Since it is assumed that there is no leakage in the system, the operational GHG emissions only refer to the annual production of CO_2 caused by the steam methane reforming and the water gas shift reaction in the fuel cell, which converts one mole of CH_4 (n_{CH_4}) into one mole of CO_2 (n_{CO_2}). The operational GHG emissions can then be calculated

$$\begin{aligned} GHG_{op,VARS+SOFC} &= m_{CO_2} = n_{CO_2} * \widetilde{M}_{CO_2} = n_{CH_4} * \widetilde{M}_{CO_2} = \frac{m_{CH_4}}{\widetilde{M}_{CH_4}} * \widetilde{M}_{CO_2} \\ &= \sum_{i=1}^{12} \dot{m}_{CH_4,i} * t_{op} * n_d * \frac{\widetilde{M}_{CO_2}}{\widetilde{M}_{CH_4}} \end{aligned} \quad (29)$$

using the molar masses of CO_2 ($\widetilde{M}_{CO_2} = 44.01\,g/mol$) and CH_4 ($\widetilde{M}_{CH_4} = 16.04\,g/mol$). For the calculation of the production-related GHG emissions, the initially required mass of NH_3 ($m_{NH_3} = 2\,kg$) (Pandya et al. 2020) and the annually required mass of CH_4 are multiplied with their respective emission factors for production ($EFP_{NH_3} = 0.840\,kgCO_2e/kg$, $EFP_{CH_4} = 0.605\,kgCO_2e/kg$) (Pandya et al. 2020).

$$GHG_{prod,VARS+SOFC} = EFP_{NH_3} * m_{NH_3} + EFP_{CH_4} * \sum_{i=1}^{12} \dot{m}_{CH_4,i} * t_{op} * n_d \quad (30)$$

For the operational cost, only the mass of methane is taken into account with a price of $c_{CH_4} = 0.88\,€/kg$.

$$C_{op,VARS+SOFC} = c_{CH_4} * \sum_{i=1}^{12} \dot{m}_{CH_4,i} * t_{op} * n_d \quad (31)$$

The investment costs take into account both subsystems ($C_{VARS} = 5{,}000$ € (Alrwashdeh and Ammari 2019), $C_{SOFC} = 15{,}000$€ (own assumption)) and the initial amount of NH_3 required ($c_{\text{NH}_3} = 0.572\,€/kg$).

$$C_{inv,VARS+SOFC} = C_{VARS} + C_{SOFC} + m_{NH_3} * c_{NH_3} \quad (32)$$

PV refrigeration system

The PV refrigeration system is composed of PV panels on the roof of the truck that generate electricity to power the compressor of a VCR system instead of the traditional diesel engine. The energy produced by the PV panels

$$E_{PV,i} = \hat{E}_{solar,i} * A_{roof} * \eta_{PV} \tag{33}$$

in a month i is calculated using the irradiation per square metre $\hat{E}_{solar,i}$ for the latitude considered in the respective scenario (see chapter "Definition of Use-Scenarios"), the area of the roof of the truck A_{roof} (it is assumed that the whole roof is covered with PV panels) and the efficiency of the PV panels η_{PV}. The values for $\hat{E}_{solar}$ are taken from a database for the year 2015 (Joint Research Centre 2015). By dividing the required cooling energy in a given scenario with the energy provided by the PV panels, the COP of the VCR system that would be required to satisfy the cooling demand is calculated.

$$COP_{req,i} = \frac{Q_{total,i} * t_{op} * n_d}{E_{PV,i}} \tag{34}$$

Because there are no other working fluids, only the refrigerant of the VCR system is taken into account for the calculation of the GHG emissions. Therefore, the operation- and production-related GHG emissions are calculated according to equation (11) and (13), respectively. The operational costs refer only to the leakage of the refrigerant and are calculated as follows:

$$C_{op,PV} = m_{ref,leak} * c_{ref}. \tag{35}$$

The investment costs include the costs for the PV panels in addition to the costs for the VCR system calculated according to equation (15). To estimate the cost of the PV panels, their kilowatt-peak-related cost ($c_{\mathrm{PV}} = 1300\ €/kWp$) (Fraunhofer ISE 2020) is multiplied with the maximum PV power in the respective scenario

$$C_{inv,PV} = C_{inv,VCR} + c_{PV} * max\left\{\frac{E_{PV,i}}{t_{op}*n_d}\right\}. \tag{36}$$

Definition of Use-Scenarios

To compare different cooling technologies, it is important to define the relevant used cases for cooled or refrigerated truck transport. For this work, eight scenarios for refrigerated transport had been developed for the comparison of the alternative technologies to the basic VCR system. For all scenarios, the general assumptions are the same and many of them are similar to the assumptions made by Venkataraman et al. (2016):

- The refrigerated trucks are operated for 20 days each month and the operating hours per day differ in the different scenarios (see Table 1).
- The refrigerated cabinet is a perfect cuboid and the door is of rectangular shape.
- There is only one door located at the back of the truck with a height of 96% of the total external height and an effective door area of 88% of the rear face.
- The external trailer dimensions (lenght $*$ width $*$ height) are:
  - $13.6\ m * 2.6\ m * 2.8\ m$ for a large truck ($40\ tons$)
  - $9.4\ m * 2.5\ m * 2.4\ m$ for a medium truck ($12\ tons$)
- The wall of the truck consists of three different layers: aluminium, Styrofoam and glass reinforced plastic (GRP) with thicknesses of $0.005\ m$, $0.125\ m$ and $0.005\ m$, respectively and thermal conductivities of $205\ Wm^{-1}K^{-1}$, $0.027\ Wm^{-1}K^{-1}$ and $0.25\ Wm^{-1}K^{-1}$, respectively.
- The thermal transmittance of the refrigerated body (k_{b}) is constant at $0.3\ Wm^{-2}K^{-1}$.
- The outside heat transfer coefficient is constant at $25\ Wm^{-2}K^{-1}$.
- All products are loaded at the refrigeration temperature (T_{r}) and the PHL is therefore equal zero.
- Heat loads from sources inside the trailer (such as lights) are not taken into consideration.
- The ratio of actual enthalpy change to maximum theoretical enthalpy change (K) is constant at 0.6.
- To represent a worst-case scenario, no shading of the trailer is considered for the calculation of the solar heat load. The solar radiation hits on the roof of the truck and one of the two side walls.

The different scenarios represent both long-distance and short-distance deliveries at two different temperature levels. Long-distance deliveries are carried out in large vehicles and are characterised by a higher average load

(X_P) and longer times between two door openings (t_{avg}). On the other hand, the duration of the door openings (θ) is comparatively long. Short-distance deliveries are carried out in medium size vehicles and have a lower average load, shorter times between two door openings and a shorter duration of door openings. For the temperatures of the cold department of the truck, temperatures of 0 °C and -20 °C are chosen. This results in four scenarios (see Table 1), which are analysed for use cases at two different latitudes (Hamburg, Germany and Catania, Italy), representing different climatic conditions, leading to eight scenarios overall.

Table 1 – Scenario Parameters

Parameter	Unit	Scenario 1	Scenario 2	Scenario 3	Scenario 4
Vehicle size	-	Large	Large	Medium	Medium
T_r	°C	-20	0	-20	0
X_P	%	85	85	40	40
t_avg	min	270	270	30	30
θ	min	8	8	3	3
t_op	h	9	9	7	7

Results and discussion

Figure 1 shows the average monthly cooling loads for the different scenarios S1-S4 in Hamburg and Catania. Scenario 1 and 3 require a greater cooling load than Scenario 2 and 4, because the refrigeration temperature is lower in S1 and S3. The maximum cooling load of 4.5 kW occurs for Scenario 3 in Catania. Generally, the cooling load in Catania is higher due to the higher external temperatures and the higher average solar irradiation. Furthermore, it can be seen that the cooling load for a refrigeration temperature of 0°C does not differ significantly between the long-distance and short-distance delivery scenario.

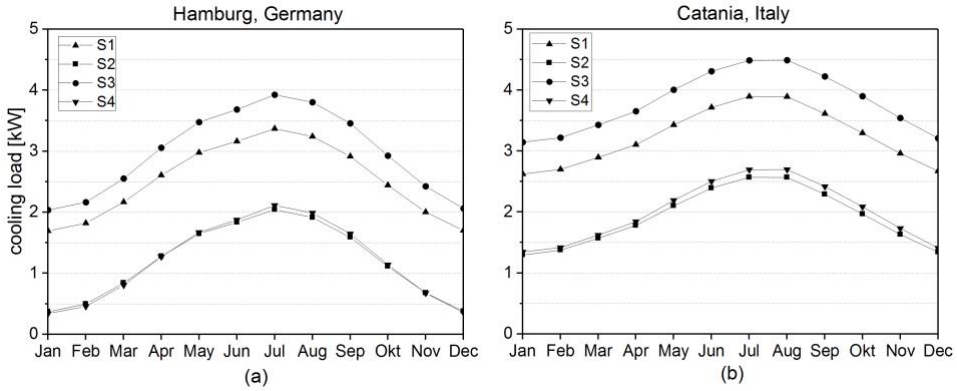

Figure 1 - Average Cooling load per month in Hamburg (a) and Catania (b) for the different scenarios

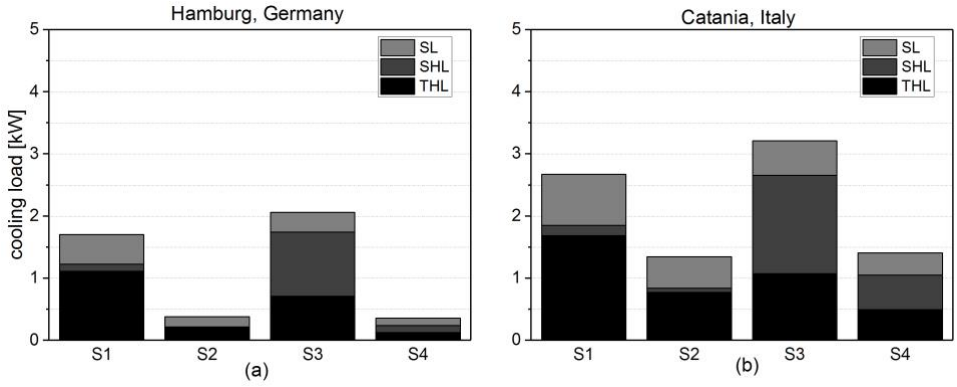

Figure 2 - Composition of cooling load in different scenarios in Hamburg (a) and Catania (b) in December

The composition of the cooling load in the different scenarios is shown in Figure 7 as an example for the month of December. The different components affect the cooling load differently in the different scenarios. For the long-distance deliveries (S1 and S2), the THL and the SL account for the largest share, because the outside area of the refrigerated cabinet is much greater for the large truck. For the short-distance deliveries (S3 and S4), the impact of the SHL significantly increases because of the frequent door openings.

The annual GHG emissions associated with the different systems are shown in Figure 3. S1 and S4 represent the scenarios with the highest and lowest GHG emissions, respectively. Although cryogenic fluids do not cause operational GHG emissions, they cause the most GHG emissions overall, as large quantities of cryogenic fluids are needed to satisfy the required cooling load and this is associated with high production-related GHG emissions. The production-related emissions of LCO_2 are 6-7 times higher than the production-related emissions for diesel in the respective scenario, which is in line with the results from Rai and Tassou (2017a). The VCR and the VARS+SOFC systems cause high operational GHG emissions, as these systems produce CO_2 directly through their energy supply by means of a diesel engine or fuel cell. The eutectic and PV systems are the most promising alternatives in terms of GHG emissions. However, it should be noted that the emissions caused by the production of the hardware were not considered for any of the systems.

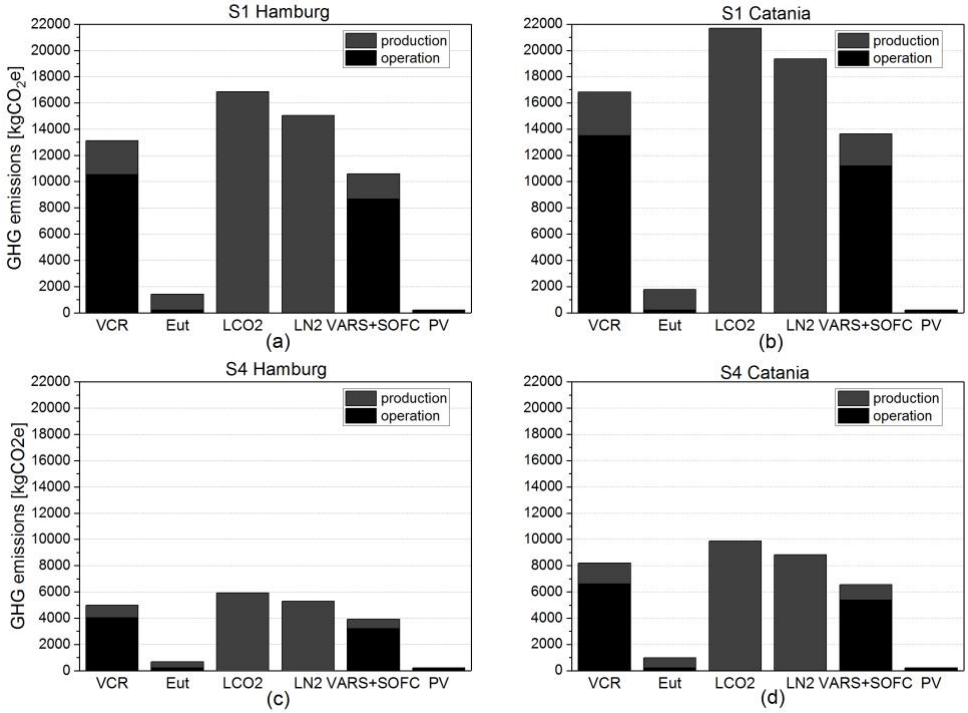

Figure 3 – Annual GHG emissions for scenario 1 in Hamburg (a) and Catania (b) and scenario 4 in Hamburg (c) and Catania (d) for the different technologies

In addition, some systems have disadvantages in terms of the security of cooling supply, as some systems have much shorter maximum operating times, which could cause problems if the delivery is delayed due to traffic jams or other reasons. The operating time of the eutectic system is limited by the size of the PCTSU and recharging requires that the truck has reached its destination to be recharged. The reliability of PV panels is highly dependent on weather conditions, whereby the use of an additional battery system can help to extend the operation time of the cooling system. Table 2 shows which COP of the PV-powered VCR system would be necessary to satisfy the required cooling load in the respective scenario. It is assumed that a COP above 2 is difficult to achieve and a COP above 2.5 cannot be achieved at all in a mobile application. Surprisingly the systems are performing better in summer than in winter. The significantly reduced solar radiation in winter has a much stronger effect compared to the higher cooling demand in summer.

Table 2 - Required COP of the PV-driven VCR system to satisfy the required cooling load

COP	Hamburg				Catania			
	S1	S2	S3	S4	S1	S2	S3	S4
Jan	2.6	0.6	3.7	0.6	0.9	0.4	1.3	0.5
Feb	1.6	0.4	2.2	0.5	1.0	0.5	1.4	0.6
Mar	0.8	0.3	1.1	0.3	0.6	0.4	0.9	0.4
Apr	0.5	0.3	0.7	0.3	0.4	0.3	0.6	0.3
May	0.6	0.3	0.8	0.4	0.4	0.3	0.6	0.3
Jun	0.5	0.3	0.7	0.4	0.4	0.3	0.6	0.3
Jul	0.6	0.4	0.8	0.4	0.4	0.3	0.6	0.3
Aug	0.6	0.4	0.9	0.5	0.5	0.3	0.7	0.4
Sep	0.9	0.5	1.2	0.6	0.6	0.4	0.9	0.5

Okt	1.3	0.6	1.8	0.7	0.8	0.5	1.1	0.6
Nov	2.4	0.8	3.5	1.0	0.9	0.5	1.3	0.6
Dec	3.0	0.7	4.3	0.7	1.0	0.5	1.4	0.6

Figure 4 shows the cumulative NPV for the different systems for S1 and S4. Since only costs are considered, but no revenues, all NPV values are negative. Accordingly, the investment that comes closest to zero is the most profitable. The PV system requires the largest investment, but since the operating costs are the lowest, this system shows a positive trend for the cumulative NPV and is the most profitable in S1 from the fourth year onwards. The cryogenic systems with LCO_2 and LN_2 have a very low NPV because, as already mentioned, they are very mass intensive to satisfy the required cooling load and thus have high operating costs. Nevertheless, they can be more profitable than the VCR system in low cooling load scenarios (S4). Furthermore, it is conceivable that the costs of alternative technologies will fall as market penetration increases.

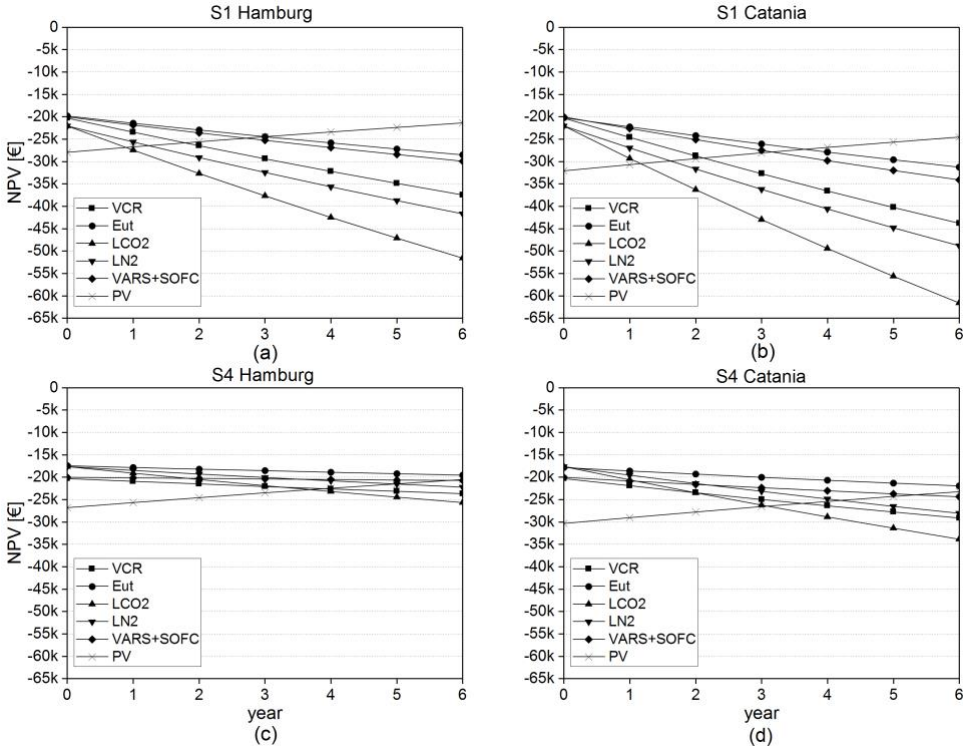

Figure 4 - Cumulative NPV for scenario 1 in Hamburg (a) and Catania (b) and scenario 4 in Hamburg (c) and Catania (d) for the different technologies

Conclusion

Cold and refrigerated transports in Europe are responsible for a significant amount of energy consumption and related emissions. The traditional cooling system driven by a diesel engine is especially inefficient when the truck is not moving. Therefore, energy efficiency measures and the use of renewable energy to reduce the energy consumption and reducing the CO_2 footprint of food transport plays a key role to reduce the emissions from the transport sector. In this work we have compared a number of alternative systems for the provision of the required cooling load. Eutectic cooling systems as well as the use of PV electricity for an electric VCR system seem to be the most promising solutions in terms of emissions and cost reduction. Challenges are arising for the PV system from the strongly fluctuating available solar electricity, which is following a clear day/night cycle and which is higher in the southern hemisphere. However, the higher solar radiation is also a backdraft to the process as higher ambient temperatures increase the cooling demand of the system. Thus, despite the higher solar gain in the south this is balanced by the lower cooling load in the northern hemisphere.

Further configuration of system can be analysed and the electrification of the whole drive train of commercial vehicles might drive the systems change further. If the main diesel tank for the drive motor is going to be replaced by electric drive trained, this will also be the case for the drive of the cooling units used on the truck.

Acknowledgment: This work was partially funded by the IAESTE student exchange program and the European Union's Horizon 2020 research and innovation programme under grant agreement No. 847040 for the Project Improving Cold Chain Energy Efficiency (ICCEE).

References

BDEW, 2021. BDEW-Strompreisanalyse Januar 2021. Bundesverband der Energie- und Wasserwirtschaft e.V.

Air Resources Board (2015) Technology Assessment: Transport Refrigerators.

Alrwashdeh, S.S., Ammari, H. (2019) Life cycle cost analysis of two different refrigeration systems powered by solar energy. Case Studies in Thermal Engineering 16:100559.

Ariyadi, H.M. Thermodynamic study on absorption refrigeration systems using ammonia/ionic liquid working pairs, 2016.

Automotive Fleet, 2015. Environmental Dangers of Global Refrigerated Transport Studied. https://www.automotive-fleet.com/129394/environmental-danger-of-global-use-of-refrigerated. Accessed 27 March 2021.

Belyadi, H., Fathi, E., Belyadi, F. (2019) Economic evaluation. In: Hydraulic Fracturing in Unconventional Reservoirs. Elsevier. pp. 341–404.

Bonaventure, M., Benchik Lehocine, A.E., Croquer, S., Huchtemann, K., Poncet, S. (2020) Heat and mass transfer in a loaded truck trailer equipped with eutectic plates: a comparative numerical study.

Brooks, K., Block, G., Lutkauskas, T. (2016) Demonstration of Fuel Cell Auxiliary Power Units (APUs) to Power Transport Refrigeration Units (TRUs) in Refrigerated Trucks.

California Air Resources Board, n.d. High-GWP Refrigerants. Accessed 24 March 2021.

Department for Business, Energy & Industrial Strategy, 2017. Greenhouse gas reporting: conversion factors 2017.

Eitner, U., Ebert, M., Zech, T., Schmid, C., Watts, A., Heinrich, M. (2020) Solar Potential on Commercial Trucks: Results of an Irradiance Measurement Campaign on 6 Trucks in Europe and USA 33.

Eriksson, M., Ahlgren, S., 2013. LCAs of petrol and diesel. Swedish University of Agricultural Sciences, Uppsala, Sweden, 38 pp.

FIC S.p.A., n.d. Interview via E-Mail. https://www.fic.com/en. Accessed 25 March 2021.

Fraunhofer ISE, 2020. Photovoltaics Report, Freiburg, Germany, 50 pp.

Garde, R., Jiménez, F., Larriba, T., García, G., Aguado, M., Martínez, M. (2012) Development of a Fuel Cell-Based System for Refrigerated Transport. Energy Procedia 29:201–207.

Honsberg, C.B., Bowden, S.G., 2019. Photovoltaics Education Website. http://www.pveducation.org/. Accessed 23 March 2021.

Joint Research Centre, 2015. Photovoltaic Geographical Information System: monthly irradiation data. https://re.jrc.ec.europa.eu/pvg_tools/en/#MR. Accessed 25 March 2021.

Kühnel, M., Hanke, B., Geißendörfer, S., Maydell, K. von, Agert, C. (2017) Energy forecast for mobile photovoltaic systems with focus on trucks for cooling applications. Prog. Photovolt: Res. Appl. 25:525–532.

Liu, M., Saman, W., Bruno, F. (2012) Development of a novel refrigeration system for refrigerated trucks incorporating phase change material. Applied Energy 92:336–342.

Mak, S.H., Mei, J., Cheng, X., Cheng, K.W.E., 2017. Solar electric refrigerator truck development program. In: 2017 7th International Conference on Power Electronics Systems and Applications. Smart Mobility, Power Transfer & Security : 12-14 Dec, 2017, Hong Kong. 2017 7th International Conference on Power Electronics Systems and Applications - Smart Mobility, Power Transfer & Security (PESA), Hong Kong. 12/12/2017 - 12/14/2017. Power Electronics Research Centre, The Hong Kong Polytechnic University, Hung Hom, Kowloon, Hong Kong. pp. 1–4.

Pandya, B., El-Kharouf, A., Venkataraman, V., Steinberger-Wilckens, R. (2020) Comparative study of solid oxide fuel cell coupled absorption refrigeration system for green and sustainable refrigerated transportation. Applied Thermal Engineering 179:115597.

Pedolsky, H., La Bau, R. (2010) Reintroduction of Cryogenic Refrigeration for Cold Transport.

Phase Change Material Products Limited, n.d. Interview via E-Mail. https://www.pcmproducts.net/. Accessed 24 March 2021.

Radebe, T.B., Huan, Z., Baloyi, J. (2020) Simulation of eutectic plates in medium refrigerated transport. JEDT 19:62–80.

Rai, A., Tassou, S.A. (2017a) Energy demand and environmental impacts of alternative food transport refrigeration systems. Energy Procedia 123:113–120.

Rai, A., Tassou, S.A. (2017b) Environmental impacts of vapour compression and cryogenic transport refrigeration technologies for temperature controlled food distribution. Energy Conversion and Management 150:914–923.

Tassou, S.A., De-Lille, G., Ge, Y.T. (2009) Food transport refrigeration – Approaches to reduce energy consumption and environmental impacts of road transport. Applied Thermal Engineering 29:1467–1477.

Thermo King, n.d. V-800 MAX product sheet. https://europe.thermoking.com/it/direct-drive/discover-the-range/v-800-max/. Accessed 24 March 2021.

Thermo King (2014) Cryotech: Single and multi temperature refrigeration system for truck & trailer.

Umweltbundesamt, 2020. Entwicklung der spezifischen Kohlendioxid-Emissionen des deutschen Strommix in den Jahren 1990-2019, Dessau-Roßlau, Germany.
Venkataraman, V., Pacek, A.W., Steinberger-Wilckens, R. (2016) Coupling of a Solid Oxide Fuel Cell Auxiliary Power Unit with a Vapour Absorption Refrigeration System for Refrigerated Truck Application. Fuel Cells 16:273–293.
Wu, X., Hu, S., Mo, S. (2013) Carbon footprint model for evaluating the global warming impact of food transport refrigeration systems. Journal of Cleaner Production 54:115–124.